



ISSN: 2454-9940



**INTERNATIONAL JOURNAL OF APPLIED
SCIENCE ENGINEERING AND MANAGEMENT**

E-Mail :
editor.ijasem@gmail.com
editor@ijasem.org

www.ijasem.org

A Comparative Analysis Of Five Level Diode Clamped And Cascaded H-Bridge Multilevel Inverter For Harmonics Reduction

Mr.V.Masthanaiah¹,D.Suma²,D.Harika³,
Assistant Professor¹,
Department of EEE,

Abstract:

Multilevel inverter configurations are a suitable candidate for medium and high power applications. This study presents a new one-capacitor-based five-level (2Vdc, Vdc, 0, -Vdc, -2Vdc) boost multilevel inverter. The single-phase version of the proposed formation has one dc-source, eight switches and one capacitor. To provide boosting ability, the inverter is operating based on charge-pump theory, where the capacitor is charging in parallel and discharging in series connections to provide a higher output voltage. The proposed configuration requires simple control tasks, and for this purpose, level-shift pulse width modulation strategy, where the reference signal is compared with four carriers, is implemented to drive the switches and generates the required pulses pattern. The developed inverter has some distinct features like the usage of only one dc-source and one-capacitor, compact size, simple control requirements and boosting ability. The system is simulated with MATLAB/Simulink and a hardware prototype is developed to verify the performance of the developed five-level configuration. The results show that the developed five-level multilevel inverter reaches the expected performance

Introduction

In order to provide an alternating current (ac) output with desired amplitude, frequency, and tiny harmonic profile, dc to ac conversion is often used in renewable energy systems. The most common electrical link between ac and dc power sources is a pulse width modulation (PWM) inverter, which may have either a two-level or a multi-level arrangement. They allow the output voltage to be adjusted in terms of amplitude, frequency, and harmonics. The ac output with diminished harmonic components is generated using multilevel inverter designs. Therefore, the benefits of multilayer inverter topologies, such as a reduced filter size and an enhanced output

waveform, were discussed at length in the literature [1- 9].

A multilevel inverter uses power semiconductors to synthesize a staircase waveform from various dc levels. Multilevel inverters provide a better harmonic profile and lower semiconductor voltage strains compared to traditional two-level inverters [10].

Adding more stages to a multilayer inverter makes its output cleaner. However, this leads to a proliferation of power semiconductors and their related driving circuitry when the levels are raised. As a result, the system is complicated and expensive. Both system dependability and performance suffer as a result [10, 11].

Many inverter setups with many levels were created.

Neutral-point-clamped (NPC), cascaded H-bridge (CHB), flying-capacitor (FC), and modular multilevel converters are some examples of these setups [12-15]. These multilevel methods may be set up to provide 3, 5, 7, or even n levels of voltage output [16].

Akira Nabae and Akagi [17] introduced the NPC inverter, a three-level diode clamped form for motor driving. Although there is just one dc-source, stability and balancing of the dc-capacitors are major concerns of this architecture. To maintain the two stacks' stability and balance when the dc-capacitors are charged by the dc-source, the voltage and current through the capacitors must be managed [18].

Stillwell and Pilawa-Podgurski [19] employed an FC multilevel converter to clamp the voltage of a single capacitor's voltage level rather using a clamping diode. The FC multilevel inverter has an advantage over the NPC version due to its phase redundancies. The FC's adaptability in charging and discharging, as well as its resistance to voltage imbalances and errors, are made possible by this characteristic. The voltage strains across the power switches and the harmonic profile are both enhanced by redundancy. However, the FC multilayer inverter has a number of limitations, including low switching efficiency [15, 18] and control complexity to manipulate the voltage of all capacitors.

The CHB multilevel converter is another kind of multilevel inverter, formed by a series connection of h-bridge inverters.

The power for each bridge comes from separate dc outlets. The inverter has a lot of leeway in fault tolerance and low power level operation after cell failure [20] due to the modularity of this structure, which is a clear benefit over neutral point and FC topologies.

Multilevel inverters come in a variety of power configurations, including scalable technology and modular multilevel

inverters. In this architecture, any number of layers may be generated by connecting a variety of submodules, each with its own control system. However, managing the modular multilevel topologies is a significant challenge due to the fact that current circulation inside the converter raises the system's total conduction losses [15, 18].

A novel five-stage boost inverter is described in this publication.

There are a variety of different five-level structures reported in the literature.

With only six switches, two diodes, and two capacitors, you can build the five-level arrangement described in [21]. There are fewer switches, but balancing the capacitors and diodes needs a sophisticated control algorithm, which reduces system efficiency. As with [21], the arrangement given in [22] is based on the switched capacitors cell; however it is intended to yield nine levels as opposed to five. Based on switched-capacitor-converters, Roy et al. [23] designed a cross-switched inverter that makes efficient use of switches; however, the five-level version of this inverter has two capacitors, which increases the control complexity. In [24], an additional five-tiered topology is proposed. To create the necessary five-level output, however, seven switches, four diodes, and two capacitors are needed.

In order to improve upon the multilayer inverter arrangements presented in [25, 26], a novel configuration is offered here. Two dcsources with varying voltage amplitudes are needed for the topologies shown in [25, 26] to create nine levels, and six dc-sources are needed for a three-phase setup. In contrast, the version described in this research only requires a single dc-source and a single capacitor to produce a full range of five different output voltages, and even in a three-phase arrangement, a single dc-source is sufficient to execute the design.

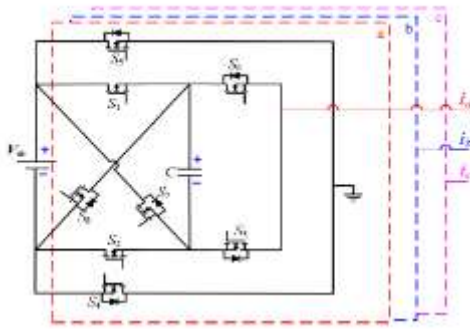


Fig. 1 General Schematic representation of proposed five-level inverter

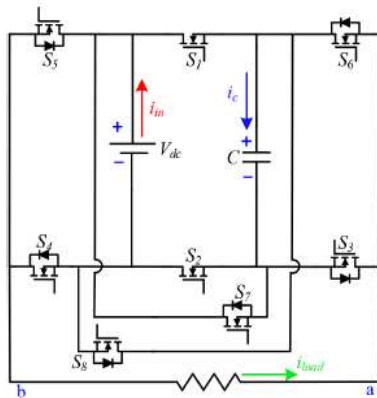


Fig. 2 Single-phase configuration of the proposed five-level inverter

Three-phase power output. The output voltage of the suggested design is more than double the input voltage, which is an advantage over the arrangement presented in [25, 26]. Using only a single dc-source, a single capacitor, and eight power switches, the suggested arrangement may provide a five-level output voltage with an amplitude twice that of the input voltage. The range of generated voltages is from $-2V_{dc}$ to $+2V_{dc}$. Figure 1 is a high-level schematic depiction of the proposed system. Adding three capacitors and 24 power switches allows the system to be scaled up to a three-phase configuration. Only the single-phase setup will be analyzed and explored here. In certain configurations, the capacitor is linked in parallel with the dc-source during charging. To get a $2V_{dc}$ output voltage level, it is disconnected from the dc-source and rejoined in series with the source. In this research, level-shift pulse width modulation (LS-PWM) is used to control the switches of a multilevel inverter. The necessary switching states are produced by

comparing the reference voltage to four carriers.

This research is structured as follows: The several modes of operation of the multilevel boost-inverter are discussed in Section 2. In Section 3, we'll go through our modulation technique; in Section 4, we'll calculate the losses brought on by our suggested setup; and in Section 5, we'll provide our findings from both simulation and experimentation.

Multilevel inverter with two proposed boost levels

In Fig. 2, we can see the five-level boost multilevel inverter that was presented. The output voltage is double the input voltage in the suggested design, which is a five-level multilevel inverter with boosting capability. Only eight switches are used in the designed topology, with two of those switches lacking an anti-parallel diode. However, only six valid switching states are implemented in order to provide the five-level output voltage, as shown in Table 1. Figures 3 and 4 show all the possible operating states.

2.1 Modes of Operation

In the first, "freewheeling," mode, the inverter outputs 0 V and the dc-source charges capacitor C (Fig. 3a). This study assumes the capacitor is charged when a big inrush current is pulled from a dead capacitor at zero voltage. In fact, this is a problem for any multi-tiered architecture that makes use of FCs. A precharge device, which permits the capacitor voltage to rise up gradually, might be used in high power applications [27-32]. The switches labeled S1, S2, S3, and S4 are all turned on. The voltage across capacitors C is the same as the voltage across the dc source since C is being charged by the dc source. The input voltage charges capacitor C, and the steady-state value of capacitor C is equal to the input voltage. The a and b output terminals are linked together.

In Mode 2, with just S1, S2, S3, and S5 activated, the inverter produces an output

voltage equal to the input voltage (Fig. 3b). The voltage across capacitors C is the same as the voltage across the dc source since both are charged from the same source. The positive terminal of the input source is linked to terminal b of the output, while the negative terminal of the dc source is connected to terminal a.

In Mode 3, switches S3, S5, and S8 are on, while the rest of the switches are off, causing the inverter to produce an output voltage that is double the input voltage (see Fig. 3c). Terminal b of the output is wired to the + terminal of the dc-source, while terminal an is wired to the - terminal of capacitor C.

In freewheeling mode 4 (see Fig. 4a), the inverter's output voltage is zero, and the dc-source charges capacitor C. The switches labeled S1, S2, S3, and S4 are all turned on. The voltage of C is identical to the voltage of the dc source since it is charged directly from the dc source. The input voltage is used to charge capacitor C, and the steady-state value of C is the same as the input voltage. The second output terminal (b) is wired to the first (a).

In mode 5, all except switches S1, S2, S4, and S6 are on, and the inverter produces an output voltage equal to the input voltage (see Fig. 4b). Voltage in C is constant since it is being charged by the dc source. Terminal b of the output is wired to the negative end of the dc source, whereas terminal an is wired to the positive end.

In mode 6, switches S4, S6, and S7 are on, while the other switches are off. This mode causes the inverter to produce an output voltage that is double the input voltage (see Fig. 4c). The positive terminal of capacitor C is linked to terminal a, while the negative terminal of the dc-source is connected to terminal b, the output.

2.2 Parameterized layout

Capacitance selection is critical to minimizing ripple voltage, since excessive ripple might result in uneven voltage steps at the output. C is charged in parallel with the dc source, as shown in Figures 3a, b,

and 4a. The resulting characteristic equations are as follows:

$$\{v_c = v_{dc} \Leftrightarrow i_c = i_{in} \tag{1}$$

The charging process for C is ongoing in the configuration shown in Fig. 4a. Its present equation, however, differs from its historical one and may be labeled as

$$\{v_c = v_{dc} \Leftrightarrow i_c = i_{in} - i_{load} \tag{2}$$

The characteristics equation of the capacitor when C is discharging in the modes shown in Figures 3c and 4b is

$$\{v_c = v_o - v_{dc} \Leftrightarrow i_c = i_{in} \tag{3}$$

Fig. 5 shows a graph showing the voltage across a capacitor. C might be chosen in the following ways based on the graph and equations (1-3):

Table 1 Switching states of the five-level inverter

Vector	S ₁	S ₂	S ₃	S ₄	S ₅	S ₆	S ₇	S ₈	Output
V ₀	1	1	1	1	0	0	0	0	0
V ₁	1	1	1	0	1	0	0	0	V _{dc}
V ₂	0	0	1	0	1	0	0	1	2V _{dc}
V ₃	1	1	1	1	0	0	0	0	0
V ₄	1	1	0	1	0	1	0	0	-V _{dc}
V ₅	0	0	0	1	0	1	1	0	-2V _{dc}

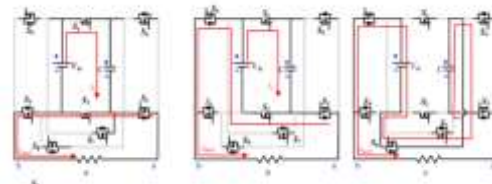


Fig. 3 Operation modes Mode I, (b) Mode II, (c) Mode III

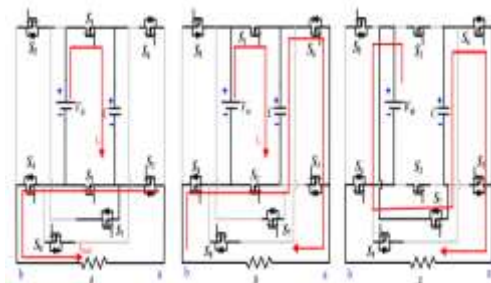


Fig. 4 Operation modes (a) Mode IV, (b) Mode V, (c) Mode VI

$$C = \left(\frac{V_o - V_{dc}}{2\Delta v_c} \right) DT_s \tag{4}$$

Input voltage v_{dc}, output voltage v_o, sampling time T_s, allowable ripple in

capacitor voltage v_c , and duty ratio D are all inputs into the equation that yields C .

Table 2 provides a summary of the component voltage and current stresses. The current pressures on each switch are about the same.

However, there seems to be a variety of voltage stressors. The largest voltage stress is seen in S_7 and S_8 , which is coincident with the output voltage. On the other switches, the voltage stress is proportional to the input voltage. The voltage strains on switches S_7 and S_8 are greater than those on the other switches because of the asymmetry in the circuit.

Therefore, component selection requires careful consideration.

PWM with a third level of level shifting
PWM is often used to control the switching frequency of power converters (dc or ac converters). Pattern of Pulses

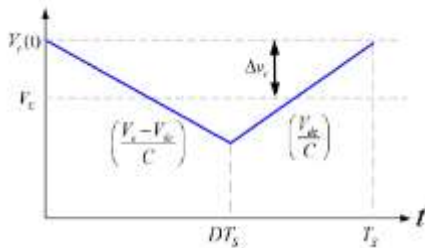


Fig. 5 Capacitor voltage illustration

The PWM block is designed to produce a waveform with a low harmonic content and a high modulation index. As an added bonus, modulation techniques may be tailored to lessen the effects of switching losses, current ripple, and capacitor voltage imbalance. The switching in a two-level converter is generated by comparing a single triangular carrier to a modulation signal.

Table 2 Devices voltage and current stress

Device	Voltage stress	Current stress
S_1	V_{in}	I_{in}
S_2	V_{in}	I_{in}
S_3	V_{in}	I_{in}
S_4	V_{in}	I_{in}
S_5	V_{in}	I_{in}
S_6	V_{in}	I_{in}
S_7	V_o	I_{in}
S_8	V_o	I_{in}

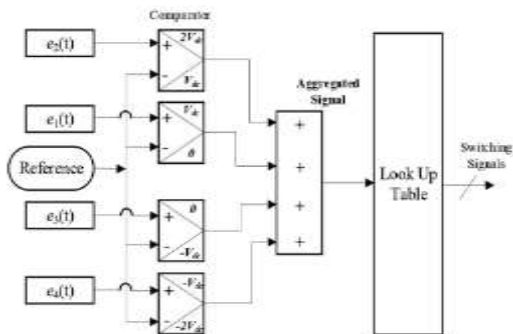


Fig. 6 Switching signal generation schematic diagram

phase-modulated signal is compared to multi-triangular carriers in multi-level topologies. Multicarrier modulation may be broken down into phase-shifted pulse-width modulation carriers and low-skew pulse-width modulation carriers.

The five-level inverter suggested here is controlled by LS-PWM produced specifically for this research. In Fig. 6, we see a schematic depicting the overarching design for how switching signals for the inverter switches are generated. N-level inverters, as stated in [33], need $(N - 1)$ different carrier waveforms in addition to a reference signal. As can be seen in Fig. 7, four carriers are used since the suggested topology has five levels. The comparison of the carrier signals to a sinusoidal reference waveform establishes the switching pattern. All four carriers have the identical amplitude, phase shift, and switching frequency for perfect symmetry. There are four distinct industries that correspond to the modulation process. Sector 1 compares the reference signal to the carrier signal e_3 , which results in an output value between 0 and V_{dc} . The output voltage in sector 2 ranges from V_{dc} to $2V_{dc}$, and is generated by comparing

the reference signal with the carrier signal e_4 . The suggested seven-stage boost converter functions symmetrically. The same method is used to depict the up half of the cycle.

The multilayer inverter's switching patterns are shown in Fig. 8.

4-Problem-solving examination of a loss

When a switching device conducts, it experiences losses known as conduction losses; when it switches, it experiences losses known as switching losses.

Each of the eight potential switching states has at least three switches activated. These results in two distinct forms of energy waste: conduction losses and switching losses. Analytical computation of switching and conduction losses will be covered in the following sections.

4.1 Losses due to conduction

Two of the eight switches in the proposed topology are power switches that can conduct in only one way while the other six can only block in one direction.

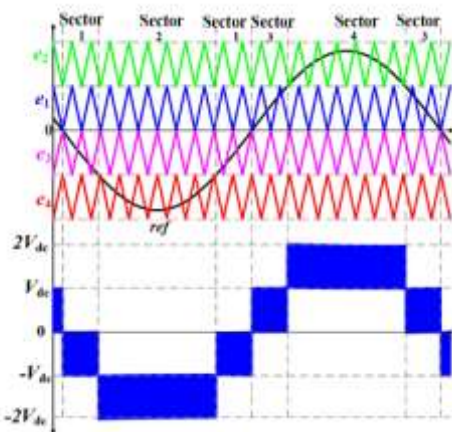


Fig. 7 LS-PWM scheme

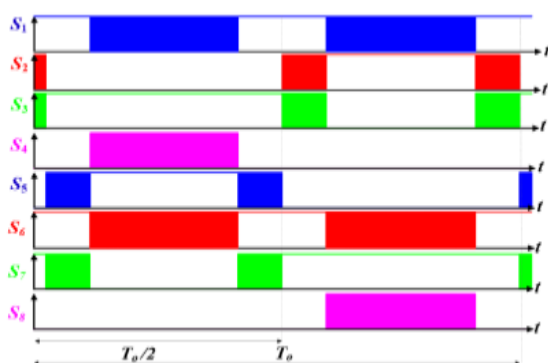


Fig. 8 Driving signals of the five-level inverter

Bidirectional conducting, the instantaneous conduction losses of the Power switch and its body diode can be given as [14, 24]

$$\rho_{c,T}(t) = [V_T + R_T i^2(t)] i(t) \quad (5)$$

$$\rho_{c,D}(t) = [V_D + R_D i(t)] i(t) \quad (6)$$

The average conduction losses are expressed as

$$\rho_{c,avg} = \frac{1}{\pi} \int_0^{\pi} \left[\{N_T(t)V_T + N_D(t)V_D\} i_c(t) + \{N_T(t)R_T i_c^{2+1}(t) + \{N_D(t)R_D i_c^2(t)\} \right] d(\omega t) \quad (7)$$

where $c,T(t)$, $c,D(t)$, V_T , V_D , R_T , R_D , N_D , N_T , and $c, avg(t)$ represent the instantaneous conduction losses of the transistor, diode, equivalent on-resistance, number of conducting diodes, number of conducting transistors, constant given by transistor characteristics, and instantaneous and average conduction losses, respectively.

Switching losses, 4.2%

A linear approximation of the switching period voltage and current may be used to determine the switching losses of each switching device [14, 24]. Losses in starting energy may be determined via the formula

$$E_{on,j} = \int_0^{t_{on}} \left[\left[V_{o,j} \frac{t}{t_{on}} \right] \left[-\frac{I}{t_{on}}(t - t_{on}) \right] \right] dt = \frac{1}{6} V_{o,j} I t_{on} \quad (8)$$

Similarly, energy losses of the j th switch during turning off are

Calculated as

$$E_{off,j} = \int_0^{t_{off}} \left[\left[V_{o,j} * \frac{t}{t_{off}} \right] \left[-\frac{I}{t_{off}}(t - t_{off}) \right] \right] dt = \frac{1}{6} V_{o,j} I t_{off} \quad (9)$$

to which $E_{on,j}$, t_{on} , I , $V_{o,j}$ $E_{on,j}$, and t_{on} represent the turn-on loss of the j th switch, the turn-on time, the switch current after turning on, the switch voltage while turning off, the turn-off loss of the j th switch, and the turn-off time.

The overall power lost while switching may be computed as

$$P_S = \sum_{j=1}^{2n+2} \left[\frac{1}{6} V_{\alpha,j} * I(t_{on} + t_{off}) f_j \right] \quad (10)$$

Fig. 9 shows a graph showing the inverter's efficiency. The suggested inverter functions well in a power range of 350 W to 650 W. However, its efficiency is more than 95% in all power ranges up to 800 W.

5 Discussions and Results

The system is simulated in MATLAB/Simulink and a hardware prototype is constructed in the lab to validate the operation in a variety of circumstances.

The Outcomes of the Simulations, Version 5.

Input voltage is kept constant at 200 V and switching frequency is maintained constant at 5 kHz throughout the simulation. The simulation framework has been used to investigate a wide variety of use cases. Figure 10 shows the connection between input current and capacitor current. It is important to remember that an inrush charging current is produced each time capacitor C is charged. Observe Fig. 10 to see this phenomena in action. As a result, the suggested topology is more suited to low-power uses.

With just one capacitor and one dcsource, the suggested topology has a clear benefit over other topologies in the literature since balancing control is unnecessary. There is no output filter between the inverter and the resistive load in Fig. 11.

Both the output voltage and current have five distinct settings (off, 0 volts, 2 volts, -2 volts, and -2 volts). As can be seen in Fig. 12, the total harmonic distortion (THD) in this instance is around 34%. Filtering it out might bring it down to a more reasonable level, even when compared to three- or even two-tiered setups.

Case study with an inductive load linked to the inverter terminals is shown in Fig. 13.

The output current is smoothed because of the inductive load, but no output filter is needed, as in the resistive load case. As can be observed in Fig. 14, the THD of the output current is around 5.14%.

5.2 Observations from Experiments

Figure 15a depicts a high-level schematic depiction of the implemented hardware setup, and Figure 15b depicts a photocopy of the actual system. The LS-PWM is implemented in DSpace 1202 to provide the gating signals for the power switches. To create the five-level multilevel inverter, eight IRFP264 power MOSFETs are employed.

In Fig. 16, we have a case study in which the input voltage is increased to 60 V and a resistive load is attached to the inverter's terminal.

The output voltage is around 120 V. Figure 17 shows the fast Fourier transform of the measured output current with a resistive load, which may be used to get the output current's total harmonic distortion (THD).

THD is below 25% without a filter, as seen in Fig. 17

The experimental waveforms of the L-R loaded prototype are shown in Fig. 18. Nothing is filtered out. Inducing a load aids in

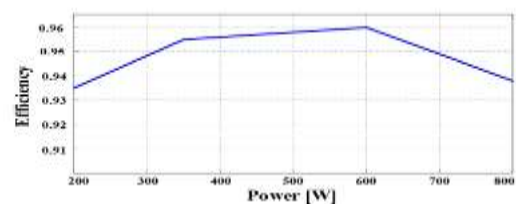


Fig. 9 Estimated efficiency of the proposed five-level multilevel inverter

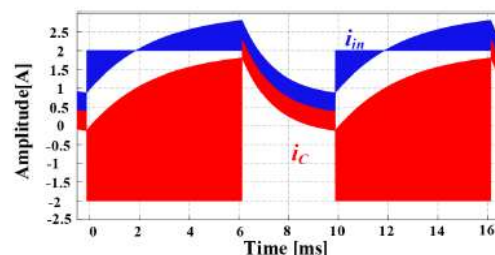


Fig. 10 Characteristics of input current and capacitor current

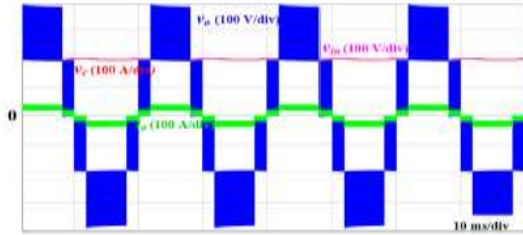


Fig. 11 Output voltage, output current, input voltage and capacitor voltage, with resistive load, $R = 200 \Omega$

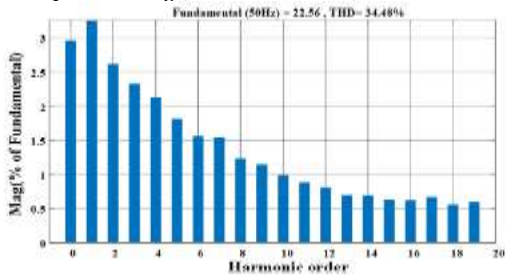


Fig. 12 THD of output current with resistive load and no filter is added

Tamp down the harmonics of the stream. THD of the output current is lowered to 8% as a result.

Table 3 shows a comparison between the suggested five-level boost inverter and other five-level topologies already available in the literature. NPC necessitates eight power switches and five capacitors but still lacks the capacity to raise voltage, leading to a lower output voltage than input. FC five-level inverters have the same number of components as NPC ones, but only need three capacitors rather of five. CHB inverters don't need capacitors, but they do need a lot of separate dc power sources. The table shows that the suggested arrangement may provide a five-level output with boosting capability, with an output voltage that is twice as high as the input voltage, and using the fewest possible parts.

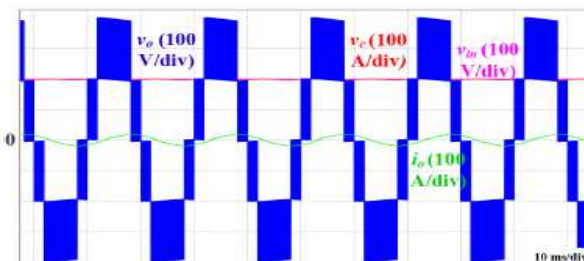


Fig. 13 Output voltage, output current, input voltage and capacitor voltage, with inductive load, $R = 10 \Omega$ and $L = 5 \text{ mH}$

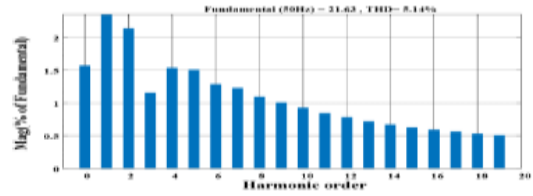


Fig. 14 THD of output current with inductive load and no filter is added

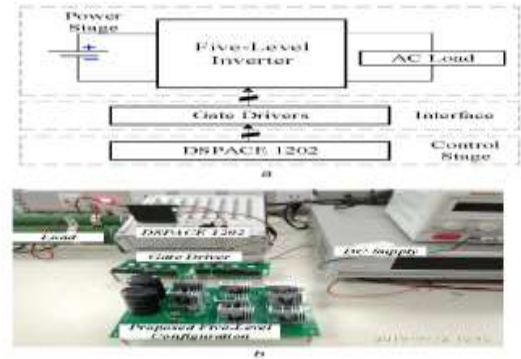


Fig. 15 Experimental setup
Block diagram, (b) Photograph of prototype

Sixthly, Wrap-Up

In this paper, a boost multilevel inverter with five stages was described. The designed arrangement for a single-phase version is made up of eight switches and a single dc-capacitor. An output of up to five levels may be produced at an amplitude more than double the input voltage. Since just one capacitor is used, there is no need to worry about the balance problem occurring.

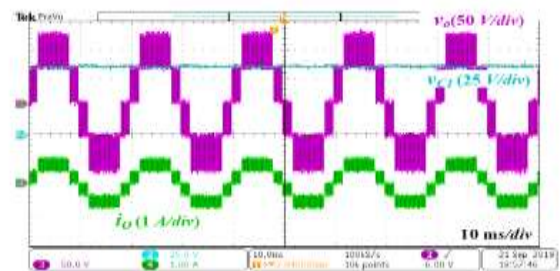


Fig. 16 Measured output voltage, output current and capacitor voltage with resistive load and no output filter, $R = 50 \Omega$

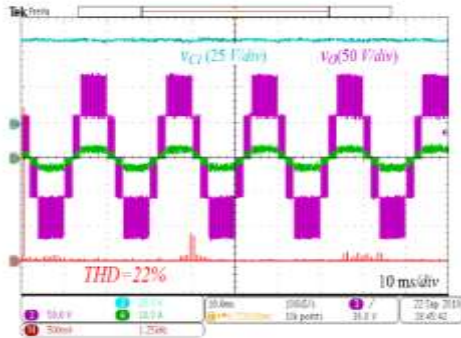


Fig. 17 Measured THD, output voltage, output current and capacitor
Voltage with resistive load and no output filter $R = 50 \Omega$

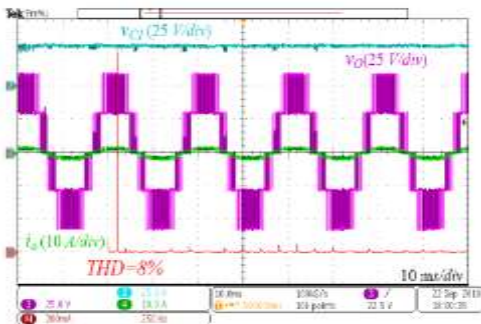


Fig. 18 Measured THD, output voltage, output current and capacitor
Voltage with inductive load and no output filter, $R = 10 \Omega$ and $L = 3 \text{ mH}$

The suggested inverter has an advantage over existing alternatives due to its boosting function, which may be used in PV systems. After being charged by the dc-source, the dccapacitor is switched into series with the power supply. This means a greater output voltage is possible. LS-PWM is used to power the inverter's switch drivers.

The switching states are planned so that the capacitor has enough time to charge, preventing significant voltage fluctuations. Table 3 Component requirements for single-phase five-level multilevel inverter

Topology	NPC [34]	FC [18]	CHB [35]	[10] [36]	Diode clamped [37]	Capacitor clamped [38]	This work
number of main switches	8	8	8	4	5	8	8
number of diodes	0	0	0	4	4	6	2
number capacitors	3	3	0	2	2	4	1
number of dc-source	1	1	2	1	1	1	1

The proposed system is tested through simulation in the MATLAB/SIMULINK environment and hardware prototyping in the lab. The analytical findings are in agreement with the simulation and experimental results.

A List of 7 Sources

[1] "Multilevel inverter topologies with reduced device count: A review," K.K. Gupta, A. Ranjan, P. Bhatnagar, et al., *IEEE Trans. Power Electron.*, 2016, 31, (1), pp. 135-151.

[2] *IEEE Trans. Power Electron.* 2017, 32(9), pp. 6677-6683 Sandeep, N., Yaragatti, U.R.: "Design and implementation of a sensorless multilevel inverter with reduced part count."

[3] A study of inverter topologies for single-phase grid-connected solar systems, Jana, H. Saha, and K. Das Bhattacharya, *Renewable and Sustainable Energy Reviews* 2017, 72, (August 2016), pp. 1256-1270.

[4] *Renew. Sustain. Energy Rev.*, 2018, 94, (November 2017), pp. 1120-1141 [5] Zeb, K., Uddin, W., Khan, M.A., et al.: "A comprehensive review on inverter topologies and control strategies for grid connected photovoltaic system." *IET Power Electron.*, 2013, 6, (8), pp. 1696-1706 Belkamel, H., Mekhilef, S., Masaoud, A., et al.: "Novel three-phase asymmetrical cascaded multilevel voltage source inverter."

[6] In 2010, Rahim and Selvaraj published "Multistring five-level inverter with novel PWM control scheme for PV application" in *IEEE's Transactions on Industrial Electronics* (Vol. 57, No. 6); in 2013, Rahim, Elias, and Hew published "Transistor-clamped H-bridge based cascaded multilevel inverter with new method of capacitor voltage balancing" in *IEEE Transactions on Industrial Electronics* (Vol. 60, No. 8), pages 2943–29 Study and analysis of novel three phase modular multilevel inverter, *IEEE Trans. Ind. Electron.*, 2016, 63, (12), pp. 7804-7813 [9] Salem, A., Ahmed, E.M., Orabi, M., et al. Single-phase 9-level hybridized cascaded multilevel inverter; I. Odeh and B. Nnadi; *IET Power Electron.*, Volume 6, Issue 3, Pages 468–477 (2013) [10] IEEE

- Transactions on Industrial Electronics, Volume 61, Issue 7 (July 2014), Pages 3269–3278 [11] Gupta, K.K., and S. Jain, "A Novel Multilevel Inverter Based on Switched DC Sources." Alishah, R.S., Hosseini, S.H., Babaei, E., et al.: "Optimal design of new cascade multilevel converter topology based on series connection of extended sub-multilevel units," IET Power Electron. 2016, 9, (7), pp. 1341-1349 [13]; Malinowski, M., Gopakumar, K., Rodriguez, J., et al. : "A Renew. Sustain. Energy Rev., 2017, 76, (March), pp. 788-812 [14]; Venkataramanaiah, J., Suresh, Y., Panda, A.K.: "A review on symmetric, asymmetric, hybrid, and single DC sources based multilevel inverter topologies." "Optimal design of new cascaded switch-ladder multilevel inverter structure," IEEE Trans. Ind. Electron., 2017, 64, (3), pp. 2072-2080 [15]; Alishah, R.S.; Hosseini, S.H.; Babaei, E.; et al. According to Prabakaran and Palanisamy (2017) in Renew. Sustain. Energy Rev., 76, pp. 1248-1282 [16], there has been "a comprehensive review on reduced switch multilevel inverter topologies, modulation techniques, and applications." 'Multilevel inverters for lowpower use,' IET Power Electron. 2011, 4, (4), pp. 384-392 [17] / De, S., Banerjee, D., Siva Kumar, K., et al. IEEE Transactions on Industrial Applications Volume I Number 5 1981, Pages 225–230 [18] Akira Nabae, I.T., and A.H. Akagi, "A new neutral-point-clamped PWM inverter." Reviews on multilayer converter and modulation approaches, Hasan, N.S., Rosmin, N., Osman, D.A.A., et al., Renew. Sustain. Energy Rev., 2017, 80, (May), pp. 163-174 [19] A five-level flying capacitor multilevel converter with integrated auxiliary power supply and start-up; Stillwell, A., and R.C.N. Pilawa-Podgurski; IEEE Trans. Power Electron. 2019; 34(3):2900-2913 [20]. IET Power Electron., 2018; 11(5):844-855 [21]; Gautam, S.P., Kumar, L., Gupta, and S.: "Single-phase multilevel inverter topologies with self-voltage balancing capabilities." Step-up switched-capacitor module for cascaded MLI topologies. Saeedian, S.M. Hosseini, and J. Adabi. IET Power Electron. 2018, 11, (7), pp. 1286-1296 [22]. IEEE Trans. Power Electron., 2018;33(8):6738-6754 [23]; Barzegarkhoo, R.; Moradzadeh, M.; Zamiri, E.; et al. ; "A new boost SwitchedCapacitor multilevel converter with reduced circuit devices." "Cross-switched multilevel inverter utilizing novel switched capacitor converters," Roy, T., P.K. Sadhu, and A. Dasgupta, IEEE Trans. IEEE J. Emerg. Sel. Top. Power Electron., 2018;6(4):2215-2226 [25]; Saeedian, M.; Hosseini, S.M.; Adabi, J.; "A five-level step-up module for multilevel inverters: topology, modulation strategy, and implementation." IET Power Electron., 2014, 7, (3), pp. 467-479 [26]; Gupta, K.K., Jain, S.: "Comprehensive review of a recently proposed multilevel inverter." IET Power Electron., 2012, 5, (4), pp. 435-446 [27]; Gupta, K.K., Jain, S.: "Topology for multilevel inverters to attain maximum number of levels from given DC sources." 'Yue yue' improved hybrid modular multilevel converter with better fault ride-through capabilities and quick pre-charging techniques, Li, Ji, Sun, et al., IET Power Electron., 2019, 12, (6), pp. 1400–1412 [28] Closed-loop precharge management of modular multilevel converters during start-Up procedures. Li, B., Xu, D., Zhang, Y., et al. [29] IEEE Trans. Power Electron., 2015, 30(2), pp. 524-531. Qin, J., Debnath, S., & Saeedifard, M.: "Precharging strategy for soft startup process of modular multilevel converters based on various SM circuits," IEEE Trans. Page numbers: 1528-1533, 2016 IEEE Applied Power Electronics Conference and Exposition (APEC), Long Beach, California. [31] Start-Up operation of a modular multilevel converter with flying capacitor submodules, IEEE Trans. Power Electron., 2017, 32(8), pp. 5873-5877 [32] - Dekka, A., Wu, B., and Zargari, N.R. Using a low-voltage DC source, Tian, Wu, Du, et al.*

provide "A simple and cost-effective precharge method for modular multilevel converters," which was published in the *IEEE Transactions on Power Electronics* in 2016. *IEEE J. Emerg. Sel. Top. Power Electron.*, 2017; 5(4):1631-1656 [34]; Wu, B.; Dekka, A.; Zargari, N.R.; et al. ; "Evolution of topologies, modeling, control schemes, and applications of modular multilevel converters." *Model Predictive Pulse Pattern Control for the Five-Level Active Neutral-Point-Clamped Inverter*, N. Oikonomou, C. Gutscher, P. Karamanakos, et al., *IEEE Trans. IET Power Electron.*, 2016, 9, (1), pp. 95-101 Hajizadeh, M., Fathi, S.H.: "Selective harmonic elimination strategy for cascaded H-bridge five-level inverter with arbitrary power sharing among the cells."

[36] 'A novel simplified multilevel inverter architecture for DC-AC conversion,' *IEEE Trans. Power Electron.*, 2006, 21, (5), pages 1311-1319 [37]; Ceglia, G., Guzmán, V., Sánchez, C., et al. "A novel hybrid voltage balance method for five-level diodeclamped converters," by D. Cui and Q. Ge, published in *IEEE Transactions on Industrial Electronics*, Volume 65, Issue 8, August 2018, Pages 6020-6031.

[38] According to He and Cheng (2016) in *IEEE Transactions on Industrial Electronics*, Volume 63, Issue 12, Pages 7814–7822, they have developed "a flying-capacitor-clamped five-level inverter based on bridge modular switched-capacitor topology."